Acta Mechanica Solida Sinica, Vol. 34, No. 6, December, 2021, 862–871 ISSN 1860-2134
https://doi.org/10.1007/s10338-021-00249-5

Novel Lightweight and Protective Battery System Based on Mechanical Metamaterials

Yao Huang[1] **Weihua Guo**[1] **Jiao Jia**[2] **Lubing Wang**[3] **Sha Yin**[1⋆]

([1] *Vehicle Energy and Safety Laboratory (VESL), Department of Automotive Engineering, School of Transportation Science and Engineering, Beihang University, Beijing 100191, China*)

([2] *Institute of Unmanned System, Beihang University, Beijing 100191, China*)

([3] *Key Laboratory Impact and Safety Engineering, Ministry of Education and Department of Mechanics and Engineering Science, Faculty of Mechanical Engineering and Mechanics, Ningbo University, Ningbo 315211, Zhejiang, China*)

Received 5 May 2021; revision received 16 June 2021; Accepted 21 June 2021;
published online 20 July 2021

ABSTRACT The challenges facing electric vehicles with respect to driving range and safety make the design of a lightweight and safe battery pack a critical issue. This study proposes a multifunctional structural battery system comprising cylindrical battery cells and a surrounding lightweight lattice metamaterial. The lattice density distribution was optimized via topological optimization to minimize stress on the battery during compression. Surrounding a single 18650 cylindrical battery cell, non-uniform lattices were designed featuring areas of increased density in an X-shaped pattern and then fabricated by additive manufacturing using stainless steel powders. Compression testing of the assembled structural battery system revealed that the stronger lattice units in the X-shaped lattice pattern resisted deformation and helped delay the emergence of a battery short circuit. Specifically, the short circuit of the structural battery based on a variable-density patterned lattice was ∼166% later than that with a uniform-density lattice. Finite element simulation results for structural battery systems comprising nine battery cells indicate that superior battery protection is achieved in specially packed batteries via non-uniform lattices with an interconnected network of stronger lattices. The proposed structural battery systems featuring non-uniform lattices will shed light on the next generation of lightweight and impact-resistant electric vehicle designs.

KEY WORDS Lightweight, Lattices, Metamaterials, Structural battery, Battery safety, Internal short circuit

1. Introduction

The development of electric vehicles (EVs) has rapidly increased in the past decade, but challenges remain associated with battery safety and driving range. It is inevitable that vehicle accidents will occur, which can result in battery explosions. Numerous studies on the mechanical integrity of lithium-ion batteries (LIBs) under mechanical abusive loading have been reported [1–4]. The internal short-circuit criterion was examined under a multiphysics coupling framework [5], while data-based

⋆ Corresponding author. E-mail: shayin@buaa.edu.cn
Yao Huang and Weihua Guo have contributed equally to this work.

machine learning was used for safety risk prediction [6, 7]. Further, multifunctional energy storage materials simultaneously possessing energy storage and load-bearing capabilities were examined as a new technology in advancing lightweight EV design. Material-level solutions such as carbon fiber-based structural batteries have been explored owing to the outstanding mechanical and electrochemical properties of carbon fibers [8–11]. Asp et al. [12–14] pioneered the fabrication of a prototype from carbon fiber-reinforced composites. Yin et al. [15, 16] focused on the design of a fiber/matrix interface to further improve the electrochemical and interfacial properties. For solutions at the system level, Siegmund et al. [17] proposed a multifunctional and damage-tolerant battery system to enhance energy storage and battery safety, whereby they combined individual cylindrical battery units and sacrificial tubes into a bimodal packing structure. That work supposed that this multifunctional battery pack would absorb energy during an impact and contribute to battery and vehicle safety. Further, this battery pack could be placed in the secondary safe zone instead of the passenger cabin where battery volume is limited. Additionally, Shuai et al. [18] designed a new thin-walled honeycomb structure for LIB packaging and developed a space mapping algorithm to optimize the entire structure for increased battery protection. Studies addressing both integrated battery protection and lightweight design are limited though in high demand.

Lattice materials are ordered cellular materials and synthetic mechanical metamaterials with mechanical properties tailored by their architecture. The structural efficiency and unusual mechanical properties of lattice materials have been widely studied during the past decade [19–22]. In addition, the corresponding multifunctional potential of lattice materials owing to the existing space inside the microstructures has been thoroughly explored [23, 24], including for heat exchange [24, 25] and impact mitigation [25, 26]. A recently proposed bi-material concept for a periodic dissipative lattice featured a bi-material lattice exhibiting high strength and strain capacity [22]. Face-centered cubic lattice materials were created featuring various rotation angles where the optimal orientation angle was identified that possessed the best energy absorption capability [27]. A multimorphology hybrid lattice was also developed whose design space for strength and energy absorption capability was expanded significantly [28]. Employing bioinspired patterning increased the energy absorption capability of dual-phase lattices to ˜2.5 times that of traditional single-phase lattices [29]. Further, optimized phase patterns produced non-uniform lattice materials with varying relative density within the design zone [30, 31].

Multifunctional lattice materials are ideal lightweight candidates for battery protection under both mechanical and thermal abusive loading. The objective of this study is to propose a structural battery concept that increases both vehicle and battery safety, featuring interconnected lattice-type metamaterials instead of sacrificial tubes [17] in the battery packing system. An optimized lattice arrangement featuring varying density is identified via topology optimization. Then, a lattice-based structural battery system with a single 18650 cylindrical battery is printed and compressed to determine the protective capability of the structure for the battery. Finally, a structural battery system with nine battery cells is examined by validated simulations

2. Design

2.1. Geometric Design

To increase the crushing safety of EV battery packs (Fig. 1a), a novel metamaterial-based structural battery system (MSBS) was developed. Figure 1b illustrates the MSBS, which featured several cylindrical batteries incorporated within interconnected lattice materials. As a representative unit comprising a single 18650 cylindrical battery, lattice units were filled into the space along the radial direction of each battery as shown in Fig. 1c. A simple body-centered cubic (that could also be generated directly from Optistruct in Sect. 2.2) cell was selected as the lattice unit, where a was the side length of lattice cell and d was the lattice truss diameter. Specifically, a was 5 mm in this study, and the side length of the entire MSBS unit was equal to 12 lattice cells (60 mm). Note that the length of the MSBS unit was 65 mm (13 lattice cells) along the axial direction of the battery dimension.

2.2. Optimal Design

The density distribution of the lattice units was optimized to obtain a minimum stress around the battery for an MSBS under lateral compression in a preliminary compression stage. A finite element (FE) model was established using solid elements in the *Hypermesh* software (*Hypermesh* 2017, Altair

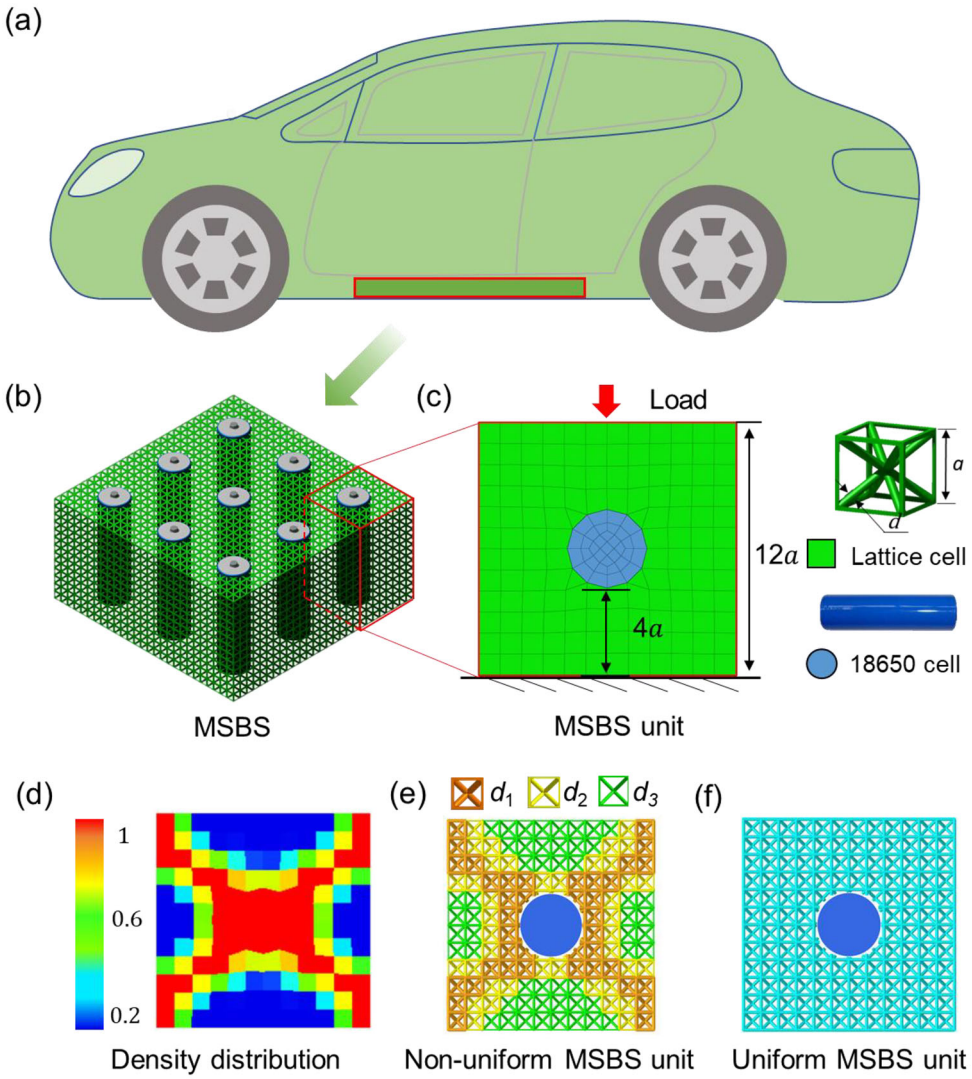

Fig. 1. Optimal design of metamaterial-based structure battery system (MSBS). **a** Schematic diagrams of new energy vehicles, **b** an MSBS and **c** an MSBS unit composed of a lattice cell and an 18650 lithium-ion battery (LIB) cell with respective geometries. **d** Optimized material density distribution. **e** Non-uniform MSBS unit. **f** Uniform MSBS unit

Engineering, Inc., USA), where the element size was set equal to a. Under lateral compression, the MSBS unit was simplified as a 2D problem to increase the computational efficiency. Then, the size of FE model along the axial battery direction was decreased to a (i.e., one lattice cell), and symmetric boundary conditions were applied. Note that FE models considering a large deformation was too complex to be used in the FE model for the complex structural battery system.

The entire optimization procedure could be divided into a topology design and a lattice layout design. The first step was to obtain the optimal density distribution of lattice units for improved battery protection. Generally two types of elements termed elements '0' and '1' exist, wherein element '0' with zero density would be deleted to achieve optimal performance with minimal mass. However, to obtain the density distribution and owing to printing precision limitations that determine a minimum truss diameter of 0.6 mm, we defined a minimum element density of 0.2. With the given design area (green area in Fig. 1c), the compression displacement was set at 1.5 mm. Furthermore, the maximum von Mises stress on the battery was used in this study as the evaluation index for battery protection capability. The optimization problem can be described as

$$\begin{aligned} &\text{Min, } S \\ &\text{Subject to, } M_f \geq 0.2 \\ &0.2 \leq X_i \leq 1 \ (i = 1, 2, ...) \end{aligned} \tag{1}$$

where S is the maximum von Mises stress on the battery, M_f is the mass fraction of the design part and X_i is the element density. All optimization parameters were set in the Optistruct software. Results are shown in Fig. 1d, which indicate that the battery should be surrounded with an X-shaped non-uniform pattern of increased density lattice units in the design area.

Next, in the lattice layout design, lattice units with different relative densities were arranged to correspond to the density variation pattern of the topological results (Fig. 1d). To simplify the layout design, lattice units with only three types of relative densities were employed, corresponding to truss diameters of 1, 0.8 and 0.6 mm (d_1, d_2 and d_3, respectively), to produce a non-uniform MSBS unit. Finally, the detailed shape near battery boundary was trimmed and the final model of a non-uniform MSBS unit was produced (Fig. 1e) and experimentally compared with a uniform MSBS unit (Fig.1f).

3. Experimental

3.1. Fabrication

The designed MSBS unit was fabricated and comprised a non-uniform lattice surrounding a single 18650 NCA/graphite cylindrical LIB. Note that all battery cells studied were fresh having undergone only a single discharging cycle to zero. The surrounding lattice was fabricated by additive manufacturing using stainless steel powders in a laser-sintering 3D printer system (EOS M280, Electro Optical Systems, Germany). The mesoscale morphology was observed via optical microscopy (KEYENCE VHX-6000 Keyence, Osaka, Japan), whereby the truss diameters of the three lattice unit types in the non-uniform MSBS unit were measured (d_1–d_3 shown as images i-iii in Fig. 2a). The diameters of the three truss types were each about 0.1 mm larger than that of the CAD model resulting in a greater relative density of the experimental MSBS unit. This discrepancy also reduced the assembly space for the LIB, so that the printed lattices required proper polishing to accommodate the LIB prior to assembly. The struts around the LIB before (image iv in Fig. 2a) and after (image v in Fig. 2a) polishing were shown.

3.2. Mechanical Testing

Quasi-static compression tests for the assembled MSBS units were carried out using in situ voltage measurements via a voltage sensor, and the compressive behavior of the non-uniform lattice MSBS units was compared with that of the uniform lattice MSBS units. To clarify the deformation mode during testing, regions with the d_3 truss diameter was painted orange. All specimens were compressed on a universal electromechanical testing machine (MTS Exceed E64, MTS Systems China, Shenzhen) at a constant crosshead strain rate of $\sim 10^{-3}$ s^{-1}. Videos of the compression tests were obtained for further analysis (Canon EOS 80D, Canon, Japan).

4. Results and Discussion

4.1. Compressive Response

A previous study [2] reported the 18650 battery performance under radial compression and validated the experimental results using finite element modeling (Fig. 2b). The compressive (engineering) stress–strain curves and in situ open-circuit voltage curves for the uniform and non-uniform lattice MSBS units are shown in Fig. 2c including the corresponding deformation history. For the uniform MSBS unit, initially the stress increased linearly until reaching the yield stress followed by a strain hardening stage with simultaneous contributions from deformation of the lattice and the LIB cell. The predominant failure mode of the uniform lattices was plastic buckling of the trusses, and the formation of an X-shaped localized shear band bypassed the LIB cell (dashed yellow line in Fig. 2d). A large deformation induced a short circuit of the LIB cell, prior to which the contributed energy absorption of the lattice cells was ~874 J. The LIB cell within the uniform MSBS unit deformed rapidly along the compression direction, also failing rapidly because of the stress concentration. The LIB voltage dropped sharply to zero at a strain of $\varepsilon = 0.15$ (Fig. 2c), which is designated as a deformation-based internal short-circuit criterion for batteries [2] and indicates the protective capability of the surrounding uniform lattice. After the short circuit of the LIB cell (at $\varepsilon > 0.15$), the lattice continued to deform considerably while

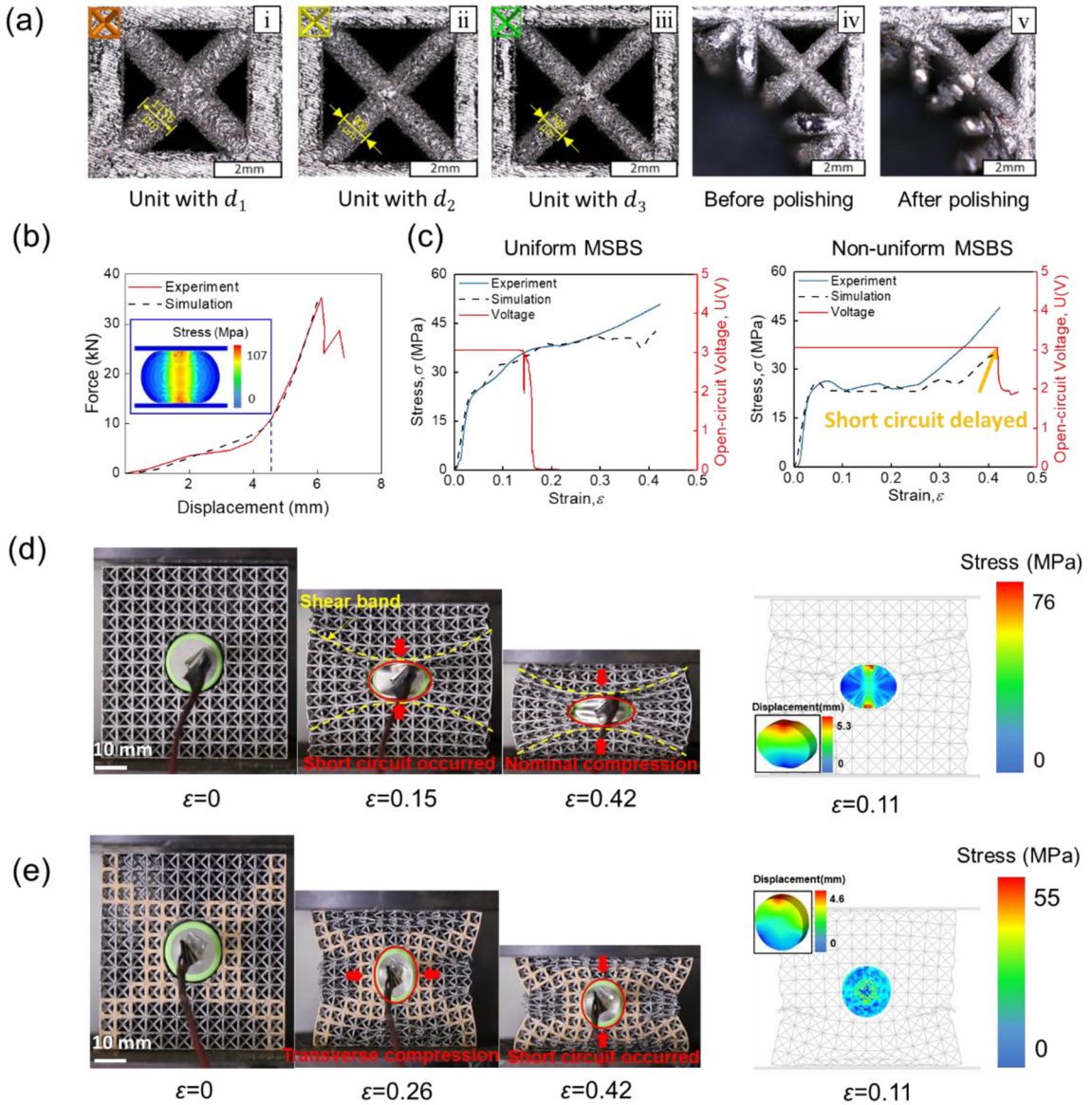

Fig. 2. Compression testing and morphology for two types of MSBSs fabricated by selective laser melting-based 3D printing. **a** Mesoscopic truss morphology images. **b** Load–displacement curves of the 18650 battery cell in radial compression by experiment (from Ref. [2]) and simulation. **c** In situ voltage curve (right axis) and engineering stress–strain curves (left axis) of uniform (left plot) and non-uniform (right plot) MSBS units. **d**–**e** Experimental and simulated deformation modes of the **d** uniform and **e** non-uniform MSBS units

the LIB cell deformed slightly. Thus, for the uniform MSBS, the stress concentration and insufficient deformation of the lattice prior to the LIB internal short circuit were responsible for its inadequate protective capability.

For non-uniform lattices, the weaker lattice cells with smaller densities (i.e., smaller truss diameters) deformed first and failed by plastic buckling of the trusses, as shown in Fig. 2e. Next, the greater density lattice units in the X-shaped pattern deformed with the surrounding weaker lattice units, resulting in a slightly horizontal compression of the LIB cell perpendicular to the loading direction with no short circuit. A long stress plateau stage occurred after the initial stress peak until the strain of $\varepsilon = 0.26$, followed by a strain hardening and lattice densification stage (Fig. 2c). The delayed short circuit of the LIB cell in the non-uniform MSBS lattice occurred at a compressive strain of 0.42, which was 166%

greater than that of the uniform MSBS unit. In the strain value range $0.26 < \varepsilon < 0.42$ strain hardening of the non-uniform lattice occurred owing to the densification of the weaker lattices, further increasing the deformation/bending of the X-shaped patterned lattices and the longitudinal compression of the LIB cell. Unlike the uniform lattice MSBS unit, the LIB cell in a non-uniform lattice MSBS underwent horizontal and then longitudinal compression during different compression stages. The stronger X-shaped patterned lattice helped resist deformation and thus helped delay the appearance of a short circuit. Prior to short circuit, the compressive stress of the non-uniform lattice MSBS unit reached 48 MPa and the absorbed energy reached 2740 J, which are 33% and 214% greater than those respective values of the uniform MSBS unit.

4.2. Simulation

Finite element analysis (FEA) was performed to further investigate the stress distribution within the LIB cell in the MSBS units during compression, using an explicit dynamics FEA approach (Radioss, Altair, USA). For an MSBS, the lattices were meshed with beam elements possessing the experimentally measured diameter, while the battery cell was meshed with solid elements. Then, the MSBS units were compressed between two stiff plates both meshed with solid elements. A mesh convergence analysis was performed to select the appropriate element size, whereby an element size of 1 mm was selected for the beam and solid elements to ensure accurate results with a high calculation efficiency. The lattice material properties were set to be ideally elastoplastic in the simulation model [29] Moreover, the battery was set as a foam model and validated by comparison with the experimental results from our previous study of a single 18650 battery cell during radial compression [2] (Fig. 2b). In this model, two types of contacts were employed. The first was a line-to-line contact that simulated the contact among lattice trusses. The second was a line-to-surface contact between the lattice trusses and the compression plates/LIB cell.

To validate the above compression model, the simulated stress–strain curves and deformation modes were compared with the experimental results of the two types of MSBS units (Fig. 2c). The simulated stress–strain curves matched well with the experiment results before densification. Furthermore, the distribution of shear bands in the lattice and the deformation of the LIB cell in the simulation results were almost the same as that observed experimentally for the two types of MSBS units. In particular, the simulated stress of the LIB cell revealed that the LIB cell stress in the uniform MSBS increased faster than that of non-uniform MSBS during the early compression stage, corresponding to an earlier short circuit of the LIB cell. Note that the local deformation induced by broken struts around the LIB cell was much smaller than the compressive deformation along the loading direction. Thus, we claim that the broken struts have little effect on the mechanical behavior herein. However, we note that the lattice design should be better optimized in future studies to avoid a possible LIB penetration by the broken lattice trusses

4.3. Variation of Multibattery Packing Patterns

Various battery packing patterns exist for battery systems that can affect the lattice arrangement in the MSBS and its battery protection capacity. A similar topology optimization process as that detailed in Sect. 2.2 was employed for a series of MSBSs containing nine battery cells and featuring different patterns. Two featured parameters, R and θ, were used to define the cell pattern (Fig. 3a). The parameter $R = r + A$, where r is the radius of the cylindrical battery and A is the radial length of the lattice structure along the length of the battery, which limited the size of the MSBS; and the parameter θ defined the specific location of each unit. Various MSBS models were established with varying values of A ($A = a$, $2a$ and $3a$) and θ ($\theta = 60°$, $90°$, $120°$, $150°$ and $180°$). From the geometric perspective, the protective area of the MSBS unit would apparently expand with increasing A, which was good for battery protection but was not conducive to a lightweight design. However, the effect of varying the parameter θ was more complex because there existed two stages of change with increasing θ value. When $\theta < 120°$, the distance between two LIBs within the same row was larger than R while the distance within each column was still equal to R. When $\theta \geq 120°$, the inter-LIB distance within each row or column was equal to R

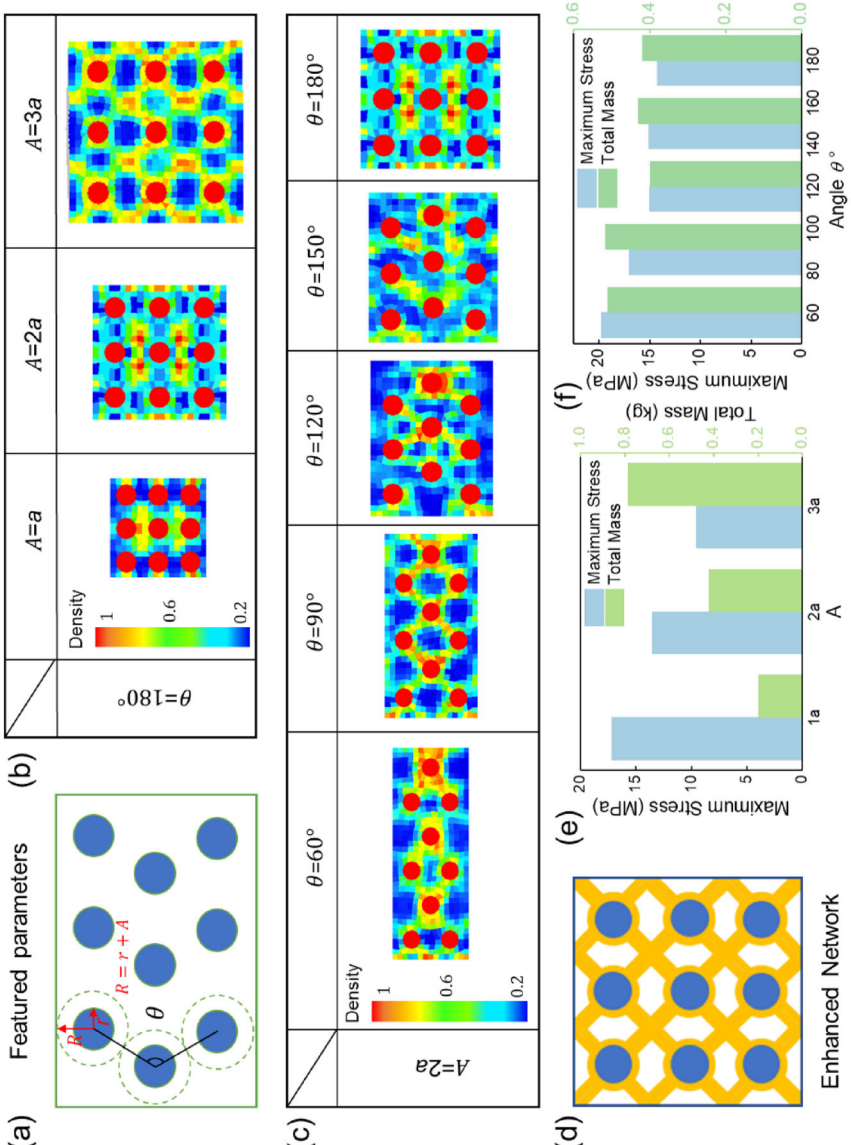

Fig. 3. Optimization design results of MSBS with battery pack. **a** Featured packing parameters for LIB cells. **b**, **c** Density distribution for MSBSs for varying (**b**) A and (**c**) θ. **d** Schematic illustration of the higher-density lattice distribution in non-uniform MSBSs. **e**, **f** Maximum stress and total mass of MSBSs for varying **e** A and **f** θ

FE models were similarly established for MSBS, but some settings were changed. To optimize MSBS with 3×3 cells, the process is described as

$$\begin{aligned} &\text{Min } \overline{S}, \\ &\text{Subject to } M_f \geq 0.2, \\ &\sigma^2 = \tfrac{1}{9}[(S_1 - \overline{S})^2 + (S_2 - \overline{S})^2 + \cdots + (S_9 - \overline{S})^2] \leq 0.02, \\ &0.2 \leq X_i \leq 1 \ (i = 1, 2, \ldots) \end{aligned} \tag{2}$$

where $\overline{S}$ is the average maximal von Mises stress of the nine battery cells and σ^2 is the variance between the real stress of each cell and the average value. The constraint of σ^2 can guarantee that all cells simultaneously possess a relatively low stress. The optimal material density distribution in the MSBS as a function of R and of θ is shown in Fig. 3b, c, respectively. Generally, stronger lattices were in the form of an X shape and featured an interconnected network among the batteries for better protection, as illustrated in Fig. 3d. The maximum battery cell stress and total MSBS mass after topology optimization are compared in Fig. 3e, f. The variation tendencies of the stress and the mass were opposite with respect to R, which is obviously owing to the incorporation of an increased amount of protective materials. Further, relatively low stress and mass values as $\theta < 120^\circ$ indicated that these MSBS were superior. For an MSBS with nine battery cells, the height h can be defined as $h = R[\sin(\theta/2) + 2]$. With smaller θ, less protective area existed along the compression direction and the growth rate was limited when $\theta \geq 120^\circ$, so that a limited amount of lattice material could be incorporated for battery protection and the stress variation was negligible. Finally, for the lightweight design of multibattery MSBSs, we recommend a battery cell patterned with $\theta \geq 120^\circ$ given by the limit of R to realize superior battery protection. Moreover, the relationship between the battery energy density per MSBS unit volume and the packing parameters R and θ can be given as

$$\rho = \begin{cases} \frac{\pi w l r^2}{4R^2(2w\cos\frac{\theta}{2}+1-\cos\frac{\theta}{2})(l\sin\frac{\theta}{2}+1-\sin\frac{\theta}{2})}, & 60^\circ \leq \theta < 120^\circ \\ \frac{\pi w l r^2}{4R^2(w+\cos\frac{\theta}{2})(l\sin\frac{\theta}{2}+1-\sin\frac{\theta}{2})}, & 120^\circ \leq \theta \leq 180^\circ \end{cases} \tag{3}$$

where w and l are the width and length of the MSBS, respectively. We should optimize the packing parameters to achieve the greatest battery density per unit volume. Accordingly, a multiobjective optimization could be employed to consider the variants all together, including the energy density per unit volume, the mass and battery protection.

5. Summary and Conclusions

A novel MSBS was proposed and a collaborative design for both a lightweight structure and battery safety was achieved via the optimization of the metamaterial density distribution. Topology optimization produced a non-uniform MSBS featuring higher-density lattices arranged in an X-shaped pattern, which were then printed and subjected to compression testing The compression test results revealed that the stronger X-shaped patterned lattices helped resist deformation and thus helped delay the appearance of a short circuit, which occurred 166% later than that of a uniform MSBS. For an MSBS containing nine battery cells, the optimized and stronger lattices formed an interconnected network among batteries that could better protect batteries from deformation. In addition, FE simulation results showed that battery MSBS cells patterned with $\theta \geq 120^\circ$ realized superior battery protection and lightweight MSBS design given by the limit of R for reduced weight and volume design. Furthermore, for actual MSBS applications, we predict that a multiobjective optimization can be employed to simultaneously consider all variables, including the energy density per unit volume, the mass and the stress. The proposed MSBS can simultaneously achieve a greater load-bearing capacity of the battery pack and superior battery protection. This is achieved by employing non-uniform lattice metamaterials with optimized density distribution and selecting the geometric packing configuration These results will inform the next generation of lightweight and safe battery system designs

Acknowledgements. The authors acknowledge financial support from the National Science Foundation of China (Nos. 11872099 and 11902015), the National Key Research and Development Program of China (2017YFB0103703) and the Fundamental Research Funds for the Central Universities, Beihang University.

Declarations

CRediT Author's Contribution YH took part in methodology, software, visualization and writing the original draft. WG was involved in software, formal analysis, investigation and writing the original draft. Ji had contributed to methodology. LW was responsible for software. SY carried out conceptualization, supervision, methodology, resources, writing, reviewing and editing.

Conflict of interest The authors declare no competing interests.

References

[1] Liu B, Jia Y, Yuan C, Wang L, Gao X, Yin S, Xu J. Safety issues and mechanisms of lithium-ion battery cell upon mechanical abusive loading: a review. Energy Storage Mater. 2020;24:85–112.
[2] Wang L, Yin S, Xu J. A detailed computational model for cylindrical lithium-ion batteries under mechanical loading: from cell deformation to short-circuit onset. J Power Sources. 2019;413:284–92.
[3] Jia Y, Yin S, Liu B, Zhao H, Yu H, Li J, Xu J. Unlocking the coupling mechanical-electrochemical behavior of lithium-ion battery upon dynamic mechanical loading. Energy. 2019;166:951–60.
[4] Wang L, Yin S, Yu Z, Wang Y, Yue TX, Zhao J, Xie Z, Li Y, Xu J. Unlocking the significant role of shell material for lithium-ion battery safety. Mater Des. 2018;160:601–10.
[5] Liu B, Jia Y, Li J, Yin S, Yuan C, Hu Z, Wang L, Li Y, Xu J. Safety issues caused by internal short circuits in lithium-ion batteries. J Mater Chem A. 2018;6:21475–84.
[6] Jia Y, Li J, Yuan C, Gao X, Yao W, Lee M, Xu J. Data-driven safety risk prediction of lithium-ion battery. Adv Energy Mater (2021).
[7] Finegan DP, Zhu J, Feng X, Keyser M, Ulmefors M, Li W, Bazant MZ, Cooper SJ. The application of data-driven methods and physics-based learning for improving battery safety. Joule. 2021;5:316–29.
[8] Kjell MH, Jacques E, Zenkert D, Behm M, Lindbergh G. PAN-based carbon fiber negative electrodes for structural lithium-ion batteries. J Electrochem Soc. 2011;158:A1455–60.
[9] Liu P, Sherman E, Jacobsen A. Design and fabrication of multifunctional structural batteries. J Power Sources. 2009;189:646–50.
[10] Kjell MH, Zavalis TG, Behm M, Lindbergh G. Electrochemical characterization of lithium intercalation processes of PAN-based carbon fibers in a microelectrode system. J Electrochem Soc. 2013;160:A1473–81.
[11] Snyder JF, Carter RH, Wetzel ED. Electrochemical and mechanical behavior in mechanically robust solid polymer electrolytes for use in multifunctional structural batteries. Chem Mater. 2007;19:3793–801.
[12] Ekstedt S, Wysocki M, Asp LE. Structural batteries made from fibre reinforced composites. Plast Rubber Compos. 2010;39:148–50.
[13] Asp LE. Multifunctional composite materials for energy storage in structural load paths. Plast Rubber Compos. 2013;42:144–9.
[14] Johannisson W, Ihrner N, Zenkert D, Johansson M, Carlstedt D, Asp LE, Sieland F. Multifunctional performance of a carbon fiber UD lamina electrode for structural batteries. Compos Sci Technol. 2018;168:81–7.
[15] Hu Z, Fu Y, Hong Z, Huang Y, Guo W, Yang R, Xu J, Zhou L, Yin S. Composite structural batteries with Co3O4/CNT modified carbon fibers as anode: computational insights on the interfacial behavior. Compos Sci Technol. 2021;201.
[16] Yin S, Hong Z, Hu Z, Liu B, Gao X, Li Y, Xu J. Fabrication and multiphysics modeling of modified carbon fiber as structural anodes for lithium-ion batteries. J Power Sources. 2020;476.
[17] Kukreja J, Nguyen T, Siegmund T, Chen W, Tsutsui W, Balakrishnan K, Liao H, Parab N. Crash analysis of a conceptual electric vehicle with a damage tolerant battery pack. Extreme Mech Lett. 2016;9:371–8.
[18] Shuai W, Li E, Wang H, Li Y. Space mapping-assisted optimization of a thin-walled honeycomb structure for battery packaging. Struct Multidiscipl Optim. 2020;62:937–55.
[19] Frenzel T, Kadic M, Wegener M. Three-dimensional mechanical metamaterials with a twist. Science. 2017;358:1072–4.
[20] Pham MS, Liu C, Todd I, Lertthanasarn J. Damage-tolerant architected materials inspired by crystal microstructure. Nature. 2019;565:305–11.
[21] Berger JB, Wadley HN, McMeeking RM. Mechanical metamaterials at the theoretical limit of isotropic elastic stiffness. Nature. 2017;543:533–7.
[22] Ruschel AL, Zok FW. A bi-material concept for periodic dissipative lattices. Mech Phys Solids. 2020;145.

[23] Evans AG, Hutchinson JW, Fleck NA, Ashby MF, Wadley HNG. The topological design of multifunctional cellular metals. Prog Mater Sci. 2001;46:309–27.
[24] Kim T, Zhao CY, Lu TJ, Hodson HP. Convective heat dissipation with lattice-frame materials. Mech Mater. 2004;36:767–80.
[25] Kim T, Hodson HP, Lu TJ. Pressure loss and heat transfer mechanisms in a lattice-frame structured heat exchanger. Proc Insr Mech Eng C-J Mech. 2004;218:1321–36.
[26] Qiu X, Deshpande VS, Fleck NA. Finite element analysis of the dynamic response of clamped sandwich beams subject to shock loading. Eur J Mech A-Solid. 2003;22:801–14.
[27] Wang P, Bian Y, Yang F, Fan H, Zheng B. Mechanical properties and energy absorption of FCC lattice structures with different orientation angles. Acta Mech. 2020;231:3129–44.
[28] Lei H, Li C, Zhang X, Wang P, Zhou H, Zhao Z, Fang D. Deformation behavior of heterogeneous multi-morphology lattice core hybrid structures. Addit Manuf. 2021;37.
[29] Yin S, Guo W, Wang H, Huang Y, Yang R, Hu Z, Chen D, Xu J, Ritchie RO. Strong and tough bioinspired additive-manufactured dual-phase mechanical metamaterial composites. J Mech Phys Solids. 2021;149.
[30] Jia J, Da D, Loh C-L, Zhao H, Yin S, Xu J. Multiscale topology optimization for non-uniform microstructures with hybrid cellular automata. Struct Multidiscipl Optim. 2020;62:757–70.
[31] Hoang V-N, Tran P, Vu V-T, Nguyen-Xuan H. Design of lattice structures with direct multiscale topology optimization. Compos Struct. 2020;252.